Characterising evapotranspiration signatures for improved behavioural insights

Hansini Gardiya Weligamage[1], Keirnan Fowler[1], Margarita Saft[2], Tim Peterson[3], Dongryeol Ryu[1], and Murray C Peel[1]

[1]Department of Infrastructure Engineering, The University of Melbourne, Parkville, Victoria, 3052, Australia
[2]Institute of Applied Geosciences, Technische Universität Berlin, 10587 Berlin, Deutschland, Germany
[3]Department of Civil Engineering, Monash University, Clayton, Victoria, 3168, Australia

Correspondence to: Hansini Gardiya Weligamage (h.gardiyaweligamage@unimelb.edu.au)

Abstract. Hydrological signatures are statistical metrics useful to quantify and infer behaviours of hydrological processes, but there has been limited use of signatures for non-streamflow variables, such as actual evapotranspiration (AET). AET signatures can assist in tasks such as evaluating remotely sensed products, diagnosing deficiencies in hydrological models, and improving understanding of hydrological processes, such as the role of AET in driving hydrological drought. This study proposes eight AET signatures defined at various temporal scales from daily to annual. We demonstrate the value of AET signatures by using them to assess two remotely sensed AET (AET_{RS}) products against flux tower AET ($AET_{Fluxtower}$) at seventeen FluxNET sites in Australia. The two AET_{RS} products are Moderate Resolution Imaging Spectroradiometer (MODIS, 16A2GFv06.1), and CSIRO MODIS Reflectance-based Scaling Evapotranspiration (CMRSET). Annually, median AET_{RS} closely matches $AET_{Fluxtower}$, except in less-arid regions. However, signatures reveal RS_{AET} largely underestimates the variability of flux tower data at both annual and monthly scales. Other monthly indices are better matched, such as indices of water stress and AET asynchronicity with potential evapotranspiration. However, some metrics are better matched in one product than the other, such as the strength and timing of seasonal fluctuations, with MODIS exhibiting a phase shift. Overall, the signatures reveal that regionally-developed CMRSET outperformed globally-developed MOD16A2GFv061. This study, the first to systematically define AET signatures, offers a way of assessing various aspects of AET dynamics across temporal scales. Furthermore, the case study highlights specific deficiencies in AET_{RS} and may assist in selecting appropriate AET_{RS}, including for modelling studies.

1 Introduction

Hydrological signatures are statistical metrics used to quantify hydrological behaviours in catchments and can be used to compare hydrological behaviour across space (Addor et al., 2018; McMillan, 2021) and to assess the behavioural fidelity of hydrological model simulations against observations (Gupta et al., 2008). Over the past decade or so, there has been rapid advancement in the application of hydrological signatures, primarily calculated based on streamflow data and related to such categories as flow magnitude, duration, frequency, timing, and rate of change (Olden & Poff, 2003). In modelling, the use of signatures contrasts with commonly used aggregate metrics (e.g., Nash Sutcliffe Efficiency (NSE) or Kling Gupta Efficiency

(KGE)), which condense the information of coherence/discrepancy between two timeseries down to a single number. In contrast, signatures retain more detailed information on different (and ideally independent) aspects of the flow regime and may

35 be used to quantify model performance to each separate aspect. Likewise, the associated hydrological processes responsible for each aspect can be separately characterised. In practice, signatures have been widely used in modelling studies (Araki et al., 2022; Kiraz et al., 2023; McMillan, 2021; Westerberg et al., 2011) , while their linking to specific hydrological processes remains an open research question, with a key challenge being the interactions among different processes to produce emergent patterns in observed data (McMillan, 2020).

40 Although there has been a wide range of hydrological signatures defined for streamflow (McMillan, 2021; Olden & Poff, 2003; Safeeq & Hunsaker, 2016), signatures directly calculated based on other hydrological processes are rare, with some notable exception of studies that used the soil moisture and groundwater signatures (e.g., Araki et al., 2022; Heudorfer et al., 2019). Therefore, in this study, we are concerned with signatures of actual evapotranspiration (AET), which have not previously been researched to our knowledge. This lack of attention to AET signatures is surprising given the importance of AET in the overall

45 water cycle, comprising around 60% of the global terrestrial hydrological cycle (Abbott et al., 2019; Teluguntla et al., 2013). While there is literature investigating and quantifying AET in different study areas, examining at different spatial scales such as in-situ level (e.g., Rungee et al., 2019), grid level (i.e., remote sensing, e.g., Zhang et al., 2010), catchment level (e.g., Avanzi et al., 2020), and regional level (e.g., Gardiya Weligamage et al., 2023), systematic and comprehensive studies focusing on AET signatures remain elusive. Moreover, some studies have used streamflow-based signatures such as total runoff ratio

50 (e.g., McMillan et al., 2014; Safeeq & Hunsaker, 2016), streamflow seasonality (e.g., Wrede et al., 2015), and diurnal cycles in streamflow (e.g., Schwab et al., 2016; Wondzell et al., 2010) to examine AET processes, although these signatures are only indirectly related to those AET processes. Furthermore, McMillan (2020) confirms that none of these streamflow-based signatures have investigated AET processes at shorter temporal scales, such as event scale.

We envisage at least three potential uses for AET signatures, namely 1) assessing the quality of remotely sensed AET products,

55 2) diagnosing deficiencies in hydrological models, and 3) improving understanding of hydrological processes. Assessment of the quality of remotely sensed AET products is important as these products are widely used across many research areas due to their ability to provide mostly continuous spatiotemporal data, unlike flux tower measurements (Yan et al., 2018; Zhang et al., 2016). However, their capacity to accurately predict various aspects of AET behaviour is often minimally assessed when incorporating them into a modelling study, and AET signatures can provide a more informative assessment. Secondly, AET

60 signatures can be employed to diagnose deficiencies in hydrological models, as the poor representation of AET could significantly impact streamflow predictions, particularly under changing climatic conditions such as climate change or multiyear droughts (Araki et al., 2022; Koster & Suarez, 2001; Peterson & Fulton, 2019). Thirdly, as noted by McMillan (2020), signatures permit extraction of "meaningful information about watershed processes", and it is often possible to define signatures to specifically provide information about a process of interest. This is particularly relevant since AET is the second

65 largest water balance component globally (after precipitation). Moreover, recent studies suggest that AET is a contributing

Hydrology and
Earth System
Sciences
Discussions

Open Access

EGU

cause to changes in rainfall-runoff relationship for the same streamflow under multiyear drought at both annual and seasonal scales (Gardiya Weligamage et al., 2023; Peterson et al., 2021).

Highlighting the importance of using AET signatures, in this paper, we define a set of AET signatures and demonstrate their use in one of the three specific contexts listed above, namely the evaluation of remotely sensed products of AET. We define

70 distinct AET signatures for various temporal scales to best capture AET characteristics relevant to each timescale. Using AET signatures, two remotely sensed products are evaluated against flux tower data at several sites covering different climatic regions in Australia.

2 Material and Methods

Given that the primary purpose of this paper is to introduce a set of signatures for actual evapotranspiration, we begin this

75 section by describing and defining the signatures themselves. This is followed by descriptions relevant to the case study, including the study area, data, and specific methods to utilise the signatures in this case.

2.1 Proposed set of signatures

We propose eight signatures to quantify AET behaviour. We do not consider this an exhaustive list but seek a set that is reasonably representative of the variety of characteristics inherent to AET dynamics as a good starting point for future research.

80 As with streamflow signatures, the metrics cover a wide range of timescales, and different metrics require different temporal aggregations of AET information (specifically daily, monthly, or annual) tailored to the metric in question.

At the annual scale, we select two signatures, namely, the *long-term median* ($\widehat{AET}_{annual}$) and interannual variability, expressed as the *coefficient of variation of annual AET* (CV_{annual}). We adopt CV rather than absolute variability measures (e.g., variance, standard deviation, or interquartile range) deliberately following streamflow signature studies such as (Clausen

85 & Biggs, 2000), as it facilitates the comparison of variability across sites with different means.

To quantify seasonal variations, we adopt two signatures: a measure of *periodicity* ($P_{12month}$) and a measure of the *timing of the seasonal peak* (TSP) in AET. The $P_{12month}$ in this study quantifies the tendency for AET variation to recur with the seasonal cycle, i.e., with a period of 12 months, and as such, is calculated as the lag-12 autocorrelation of monthly AET. This will be unity in cases where the timeseries data varies with a perfectly repeating seasonal cycle. The TSP is determined from

90 monthly timestep data by examining the median AET for each of the 12 calendar months and identifying the month with the maximum median AET. Note that the selection of median over mean AET is intended to minimize the influence of extreme values.

At the monthly scale, the monthly variability is quantified using the *monthly CV* ($CV_{monthly}$). Moreover, we define two signatures related to water stress, with the idea that the absence of water stress leads to AET perfectly mimicking potential

95 evapotranspiration (PET). When AET deviates from PET, it marks a deficit in water availability, which may be temporary (e.g., seasonal) or prolonged (as would be seen in arid environments). Both these water stress indices assume that the user has

access to a timeseries of estimated PET. The first such water stress metric, the *water stress* (WS) is defined as the difference between average monthly PET and average monthly AET, divided by the average monthly PET. Thus, higher values of this water stress signature indicate less rainfall and/or high PET. Initial testing revealed this metric to be very sensitive to aridity,

100 since it is obvious that AET will be much less than PET in arid areas. In non-arid areas, there might arise temporary (seasonal) water deficits that are not well characterised by the first water stress metric; thus, a subsequent metric was defined to these temporary fluctuations in water stress. This second water stress signature is purely based on the asynchronicity between normalised PET and AET, and thus is referred to as '*AET asynchronicity to PET*' (AAP). This latter signature can be thought of as quantifying the area between the normalised curves. It is calculated as follows. PET and AET monthly timeseries are first

105 normalised by dividing them by their mean monthly PET and AET values respectively. Then, the numerator is calculated by integrating the absolute difference between normalised monthly PET and AET ($\int(|normPET_{month} - normAET_{month}|)\,dt$). The denominator of the metric is then calculated by summing the maximum value among normalised PET and AET at each monthly time step ($\int \max(normPET_{month}, normAET_{month})\,dt$). The rationale behind calculating the absolute difference between values is that a difference between the curves is indicative of asynchronicity, regardless of which of the curves happens

110 to be greater at the given point in time.

In addition to annual, seasonal and monthly dynamics, the event scale is also important, even though it is assessable only for certain data types (e.g., flux tower data; simulations from daily timestep models) and not others (e.g., remotely sensed information provided on timesteps greater than a day). To assess AET dynamics at the event scale, we explored several options to quantify AET responsiveness to a rainfall event – in other words, the degree to which a rainfall event causes a jump in AET.

115 However, the difficulty of such a metric is that rainfall events may not only influence AET on the given day but also influence AET in the following days. If so, a standard correlation measure would be insufficient, but a lagged correlation is difficult to define since we do not know the lag a priori (and it may change over time). Seeking a generalisable metric, we select rainfall events greater than a threshold and identified the maximum daily AET value after the given rainfall event, up to a certain window duration (in days) after that event. We then apply a standard linear correlation equation to the anomalies of these

120 ordered pairs of numbers (i.e., rainfall anomaly versus maximum AET anomaly in the window after the rainfall event). Since this formulation is different from commonly used correlation metrics, we call it simply the '*Index of AET responsiveness to a rainfall event*' (R). For the purposes of the demonstration, we subjectively set the rainfall threshold and window duration parameters as 5 mm/day and 10 days, respectively. It is noted that this window size is also sensitive to the gap between selected rainfall events. If two rainfall events exceeding 5mm/day occurred within the 10-day window period, the window size is

125 restricted to the days between the two rainfall events, and the maximum AET value was chosen from that restricted window. Table 1 summarises the proposed eight signatures.

2.2 Study Area

Relative to global averages, Australia is a dry continent with annual average precipitation below 450 mm/year (Isaac et al., 2017). However, the coastal areas from southeast Australia to northern Australia receive comparatively higher precipitation,

130 exceeding 1000 mm/year in many areas. This study focuses on seventeen OzFlux sites in Australia (Figure 1). OzFlux, a part

of the international FluxNET program, is a micrometeorological monitoring network in Australia and New Zealand equipped

Table 1: AET signatures

| Temporal scale	Signature	Mathematical formulation
Annual	1. Long-term Median $(\widetilde{AET}_{annual})$	*Median of annual AET*
	2. Interannual Variability (CV_{annual})	$CV_{annual} = \dfrac{\sigma_{AET_{annual}}}{\overline{AET}_{annual}}$
Seasonal (calculated using monthly timestep data)	3. Periodicity $(P_{12month})$	*Lag 12 auto correlation of monthly AET*
	4. Timing of Seasonal Peak (TSP)	*month with maximum median of monthly AET*
Monthly	5. Monthly Variability $(CV_{monthly})$	$CV_{monthly} = \dfrac{\sigma_{AET_{month}}}{\overline{AET}_{month}}$
	6. Water Stress (WS)	$WS = \dfrac{\overline{PET}_{month} - \overline{AET}_{month}}{\overline{PET}_{month}}$
	7. [a]AET asynchronicity to PET (AAP)	$AAP = \dfrac{\int (|normPET_{month} - normAET_{month}|)\, dt}{\int \max(normPET_{month}, normAET_{month})\, dt}$
Event-scale	8. Index of AET responsiveness to a rainfall event (R)	$R = \dfrac{\sum P_{anom_{event}} * AET_{anom_{event}}}{\sqrt{\sum P_{anom}{}^2 \sum AET_{anom}{}^2}}$ where, $P_{anom_{event}} = Rainfall_i - \overline{Rainfall_i}$ $AET_{anom_{event}} = AET_{i+j} - \overline{AET_{i+j}}$ i is the position of the rainfall event, and j is the day with maximum AET after the rainfall event, $0 \le j \le 10$

[a]Note that the trapezoidal integration was conducted.

with eddy covariance measurement, providing information on carbon, energy, and water exchange. The seventeen sites

135 constitute the majority of flux towers in Australia; while seven other active flux towers exist, they were excluded due to

insufficient coverage (i.e., < 7 years) and considerable percentages of negative and unavailable data. The selected study sites

cover a wide range of climate and ecosystem regions in Australia, as summarised in Table 2. The time period of data availability

varies at each site (typically 7-20 years). Hence, different periods of data coverage are adopted in this study to perform the

analysis at each site.

140
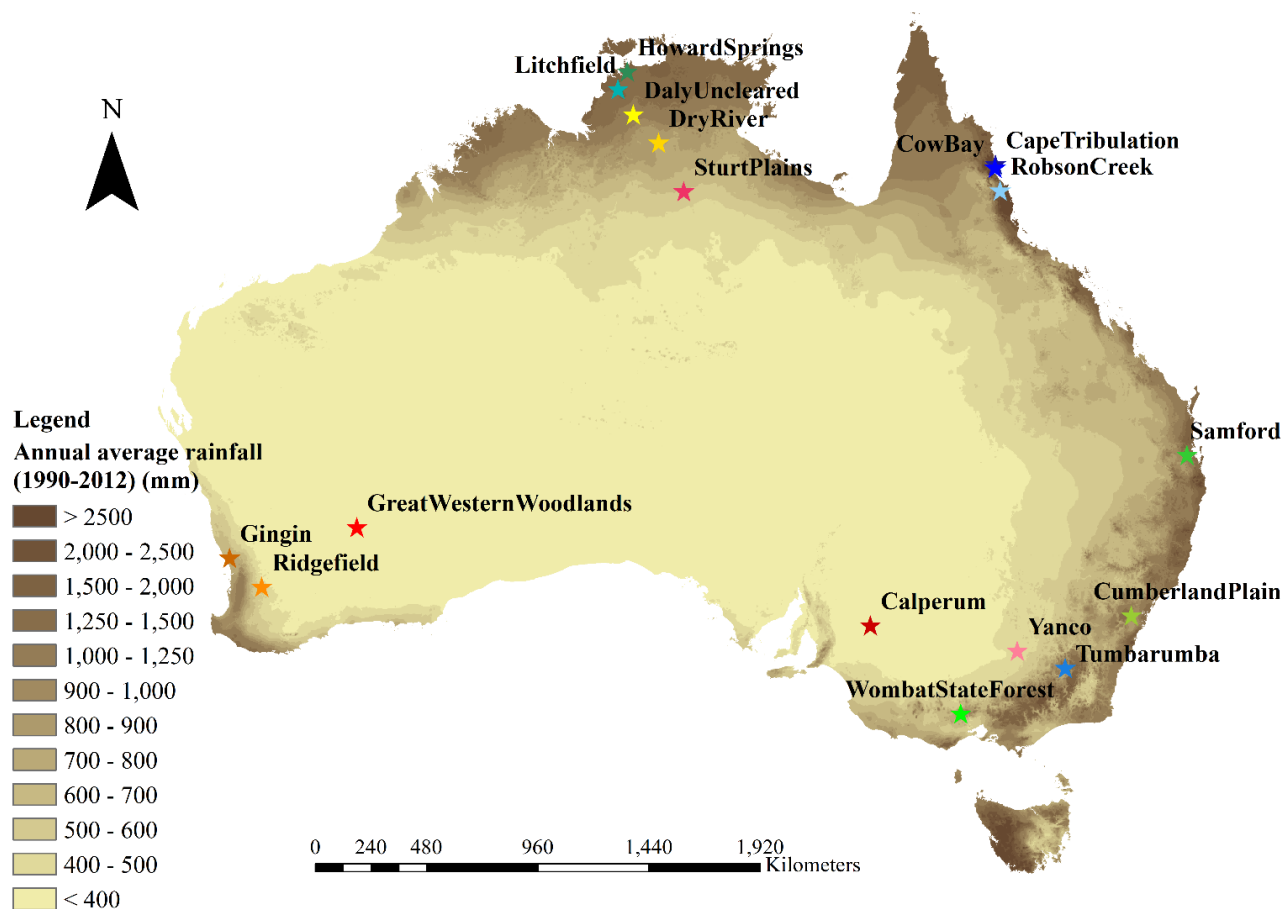
Figure 1: Locations of selected OzFlux sites in this study.

Table 2: Summary of OzFlux sites

Site	Lon.	Lat.	Data coverage[a]	Köppen Climate[b]	Eco-region[b]	Arid-ity[c]	Data source
Calperum	140.587	-34.003	Jul-10 to Feb-24	Arid desert cold	Mediterranean woodlands	4.99	(Meyer et al., 2024)
Great Western Woodland	120.654	-30.191	Jan-13 to Jan-24	Arid desert hot	Mediterranean woodlands	4.80	(Macfarlane et al., 2024)
Sturt Plains	133.350	-17.150	Aug-08 to Feb-24	Arid steppe hot	Tropical grasslands	3.18	(Beringer, Hutley, et al., 2024e)

Hydrology and
Earth System
Sciences
Discussions

Open Access

EGU

Yanco	146.290	-34.987	Jan-13 to Feb-24	Arid steppe cold	Temperate grasslands	3.14	(Beringer, Walker, et al., 2024)
Ridgefield	116.966	-32.506	Jan-16 to Feb-24	Temperate dry, hot summer	Mediterranean forests woodlands and shrub	2.95	(Beringer, Lardner, et al., 2024)
Gingin	115.713	-31.376	Oct-11 to Feb-24	Temperate, dry, hot summer	Mediterranean woodlands	2.29	(Silberstein et al., 2024)
Dry River	132.370	-15.258	Oct-09 to Feb-24	Tropical savanna	Tropical savannas	2.20	(Beringer, Hutley, et al., 2024b)
Daly Uncleared	131.388	-14.159	Jan-08 to Dec-23	Tropical savanna	Tropical savannas	1.75	(Beringer, Hutley, et al., 2024a)
Cumberland Plains	150.723	-33.615	Jan-14 to Dec-23	Temperate, no dry season, hot summer	Temperate woodlands	1.57	(Pendall et al., 2024)
Samford	152.877	-27.388	Jun-10 to Dec-17	Temperate no dry season, hot summer	Temperate broadleaf and mixed forest	1.36	(Grace et al., 2024)
Wombat State Forest	144.094	-37.422	Jan-10 to May-21	Temperate, no dry season, warm summer	Temperate broadleaf forest	1.20	(Arndt et al., 2024)
Howard Springs	131.152	-12.495	Jan-02 to Aug-22	Tropical savanna	Tropical savannas	1.17	(Beringer, Hutley, et al., 2024c)
Litchfield	130.794	-13.179	Jun-15 to Dec-23	Tropical savanna	Tropical savannas	1.17	(Beringer, Hutley, et al., 2024d)
Robson Creek	145.630	-17.117	Aug-13 to Dec-23	Temperate, dry winter, hot summer	Tropical and sub-tropical moist broadleaf forests	0.98	(Liddell & Weigand, 2024c)
Tumbarumba	148.151	-35.656	Jan-02 to Dec-22	Temperate no dry season, warm summer	Temperate broadleaf and mixed forest	0.89	(Stol & Kitchen, 2024)
Cow Bay	145.427	-16.238	Jan-09 to Jul-23	Tropical rainforest	Tropical and sub-tropical moist broadleaf forests	0.55	(Liddell & Weigand, 2024b)
Cape Tribulation	145.446	-16.103	Jan-10 to Nov-18	Tropical rainforest	Tropical and sub-tropical moist broadleaf forests	0.42	(Liddell & Weigand, 2024a)

[a]This study used version 1 of the year 2024 (2024_V1) of flux tower data from TERN data portal.

[b] Guerschman et al. (2022).

[c]Aridity refers to the aridity index defined as the ratio of potential evapotranspiration (PET) to precipitation (P).

2.3 Data

2.3.1 OzFlux eddy covariance evapotranspiration data

150 AET data, version 1 of the year 2024 (2024_V1), were obtained from OzFlux towers through the Terrestrial Ecosystem Research Network (TERN) data portal (https://portal.tern.org.au/, last accessed on 30/04/2024) at daily, monthly, and annual time scales. To minimize variability among sites due to different processing steps, the data providers consistently apply PyFluxPro (v3.4.17) to implement a standardized method to process data, as described in (Isaac et al., 2017). Level 6 flux tower data, adopted here, undergoes quality control, gap filling, and partitioning of the net ecosystem exchange of carbon

155 (NEE) data into gross primary production (GPP) and ecosystem respiration (ER). We conducted further data quality checks of the daily AET data and filtered out negative daily AET values. The maximum percentage of negative daily AET values among seventeen study sites was less than 2.3%.

2.3.2 Remotely sensed evapotranspiration data

Remotely sensed AET (AET_{RS}) products are popular due to the relative rarity of flux towers and because they provide spatially

160 distributed data, in contrast to flux tower data, which are near-point scale. Here, we present an example of the application of AET signatures to examine two AET_{RS} products to assess their ability to capture different aspects of AET behaviours at various temporal scales. The two AET_{RS} products are 1) Pixel resolution 500 m, gap filled, 8 days composites of version 6.1 of Moderate Resolution Imaging Spectroradiometer (MOD16A2GF.061) from Running et al. (2021), referred to as 'MODIS AET' hereafter, and 2) 30 m high-resolution, monthly composites of CSIRO MODIS Reflectance-based Scaling

165 Evapotranspiration (CMRSET) from McVicar et al. (2022). The MODIS AET product is one of the most widely used global AET datasets in hydrological and biogeochemical studies (e.g., Baker et al., 2021; Gaona et al., 2022; Salazar-Martínez et al., 2022), while CMRSET is an Australian regional product tested and used extensively over the corresponding region (e.g., Doody et al., 2023; Guerschman et al., 2022; Xu et al., 2022). In both cases, we extracted AET timeseries from pixels that contain the flux tower sites. The 8-day composites of MODIS AET data were aggregated into monthly data through weighted

170 temporal averaging.

2.3.3 Potential evapotranspiration data

As *water stress* and *AET asynchronicity to PET* require a timeseries of PET, they were quantified using monthly Morton's wet environment potential evapotranspiration (Morton, 1983) from the SILO (Scientific Information for Land Owners) database (https://www.longpaddock.qld.gov.au/silo/).

2.4 Method

To characterise the performance of AET_{RS} products, the signatures described in Section 2.1 are calculated separately for flux towers AET ($AET_{Fluxtower}$) and AET_{RS}. Then, we investigated the deviation of AET_{RS} signatures from $AET_{Fluxtower}$ signatures. As mentioned above, different periods have been considered at each flux tower site depending on their data coverage. For each site, the flux tower period of record determined the period of comparison between flux tower and remotely sensed information. Finally, the traditional efficiency metrics such as NSE, KGE, and components of KGE were calculated using monthly MODIS and CMRSET AET at each flux tower site in order to assess predictive skills and the challenges associated with using these traditional metrics compared to AET signatures.

3 Results

The AET signature results are presented in the four main categories based on the temporal scales in the order of 1) annual, 2) seasonal, 3) monthly, and 4) event-scale. To allow better contextualisation of AET signature results, we first present some example monthly timeseries plots of $AET_{Fluxtower}$, AET_{RS}, SILO rainfall, and PET at six flux towers (Figure 2). These timeseries plots highlight some aspects of AET that can be observed through visual inspections, such as AET variability, periodicity, and asynchronicity between AET and PET, which can subsequently be considered in AET signature results.

3.1 Annual AET signatures

Figure 3a shows an increase in the *long-term median* ($\widehat{AET}_{annual}$) values with decreasing aridity index, as expected. For example, less arid sites (shown in blues), such as Cape Tribulation and Cow Bay, have higher $\widehat{AET}_{annual}$, while more arid sites (shown in reds), such as Calperum and Great Western Woodland have lower $\widehat{AET}_{annual}$. The comparison of signatures between flux tower and RS products shows that AET_{RS} products tend to underestimate $\widehat{AET}_{annual}$, except for less arid flux sites (i.e., aridity index <1 as in Table 2), such as Robson Creek, Cow Bay, and Cape Tribulation. Readers should bear in mind the difference in the spatial footprint of data (i.e., support), which is typically on the order of 10^2-10^4 meters in the case of remotely sensed data (depending on the source, except high-resolution AET products developed based on AET sources such as Landsat and Sentinel-2), and approximately one order of magnitude smaller for flux towers (Chu et al., 2021; Finnigan, 2008). While some AET signatures may be relatively insensitive to this difference in the spatial footprint of data, it is reasonable to expect that the long-term average or median values may be sensitive to the position of the flux tower in the landscape, and thus, some variation in Figure 3a may be directly attributable to this.

Figure 3b shows a higher *coefficient of variation of annual AET* (CV_{annual}) at arid flux tower sites such as Calperum, Sturt Plains, and Yanco, whereas other sites show lower CV_{annual} within the range of 0-0.2. CV_{annual} is lower in both MODIS and CMRSET AET compared to flux towers at almost all flux towers, and the scatter is high, implying the representation of year-to-year variability is poor in MODIS and CMRSET compared to the actual inter-annual variability as seen in flux tower data.
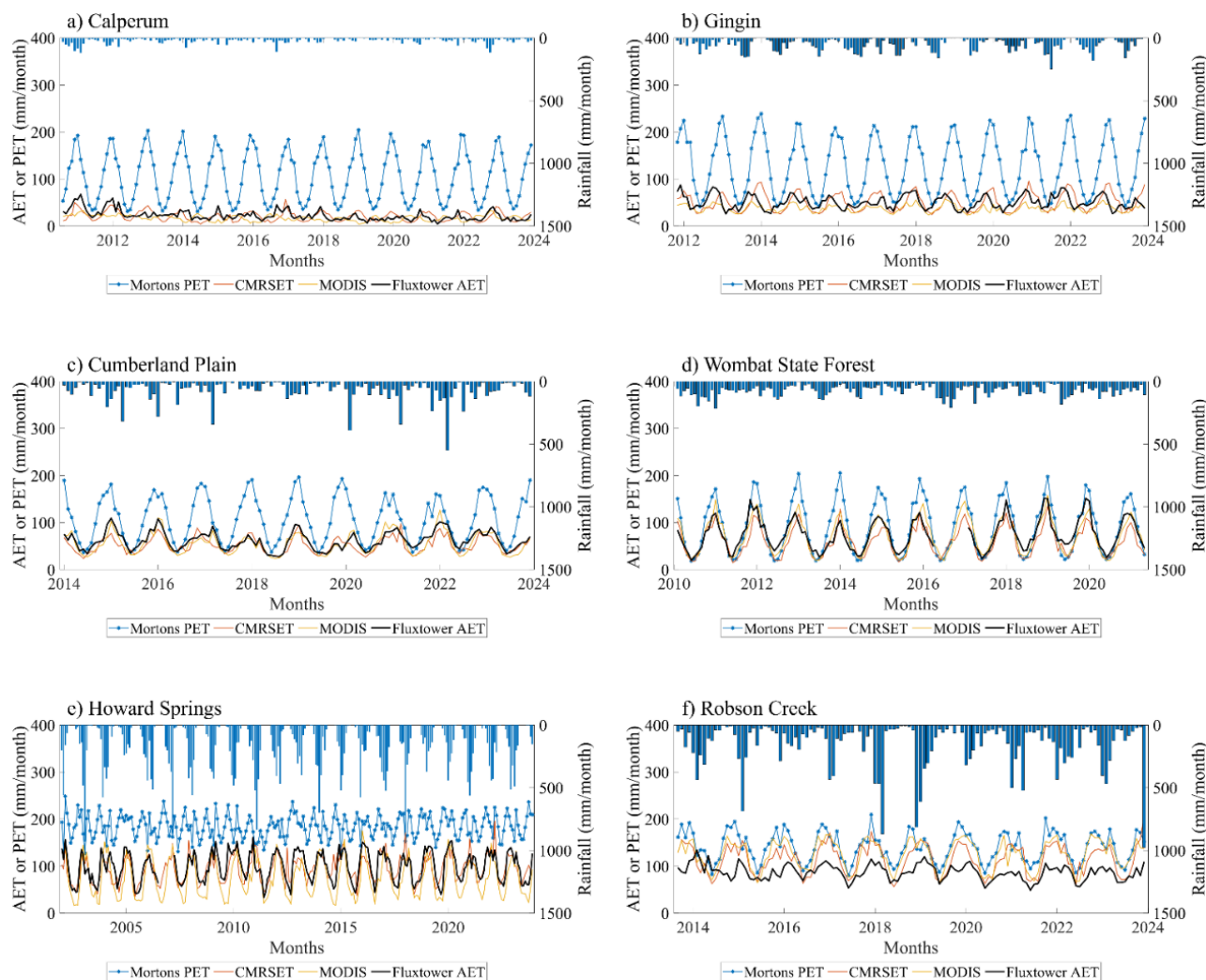
Figure 2: Monthly timeseries plots of flux tower and remotely sensed AET, rainfall and PET at six example flux tower sites.
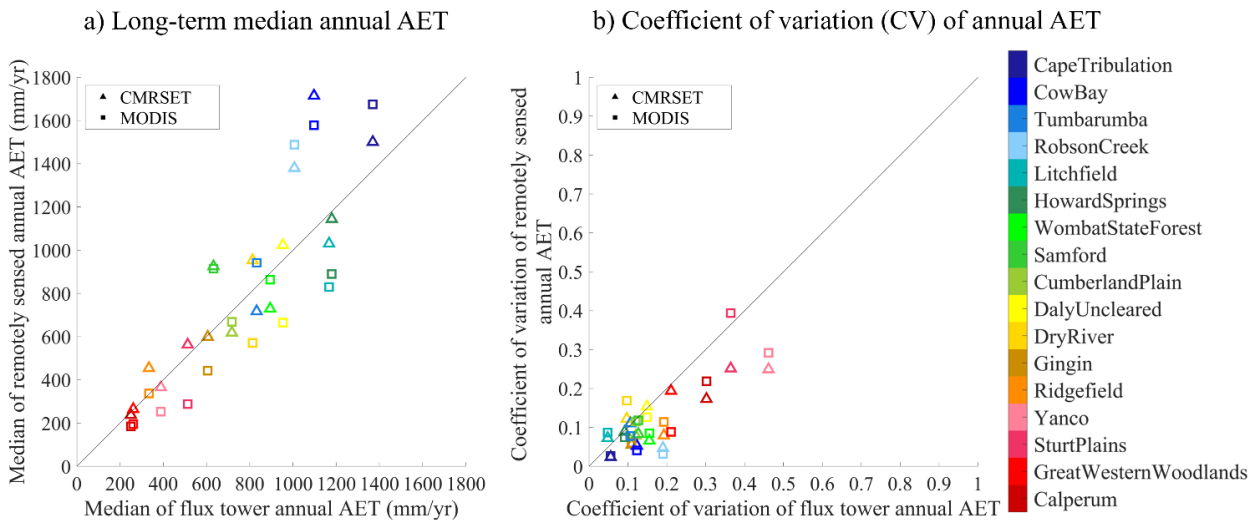
3.2 Seasonal AET signatures

Figure 4a shows *periodicity* ($P_{12month}$) via the lag-12 autocorrelation. No clear relationship is observed in $P_{12month}$ with aridity. For example, weaker $P_{12month}$ values are observed at both the more arid flux tower sites (e.g., Great Western Woodlands, Yanco) and less arid flux tower sites (e.g., Cape Tribulation). This result may reflect hydroclimatic factors since strongly seasonal climates can occur in both arid and temperate environments. Remotely sensed data performs more poorly in this metric than in any other. The $P_{12month}$ of CMRSET monthly AET shows significant scatter but minimal bias. However, MODIS monthly AET shows stronger periodic behaviour than ground measurements at most of the flux tower sites.

Figure 4b compares the *timing of seasonal peaks* (*TSP*) between AET_{RS} and $AET_{Fluxtower}$ estimates. Here, CMRSET tends to show the same timing (7 out of 17 flux towers) or closer timing (e.g., one month offset - 6 out of 17 flux towers) of *TSP* as

flux towers at many flux tower sites, whereas those calculated using MODIS AET are significantly offset with flux tower *TSP*. This confirms that CMRSET tends to capture flux tower AET seasonal peaks more closely than MODIS AET. The MODIS results for these two metrics suggest that strongly periodic remote sensing estimates do not necessarily align well with the *TSP* in ground measurements (i.e., $AET_{Fluxtower}$).

Figure 3: Comparison of annual AET signatures; a) Long-term median AET, b) Coefficient of variation (CV) of annual AET, between remotely sensed AET (MODIS and CMRSET AET) and flux tower AET. (Note that the flux towers are ordered by aridity index – from Cape Tribulation (Lowest aridity) to Calperum (Highest aridity)).
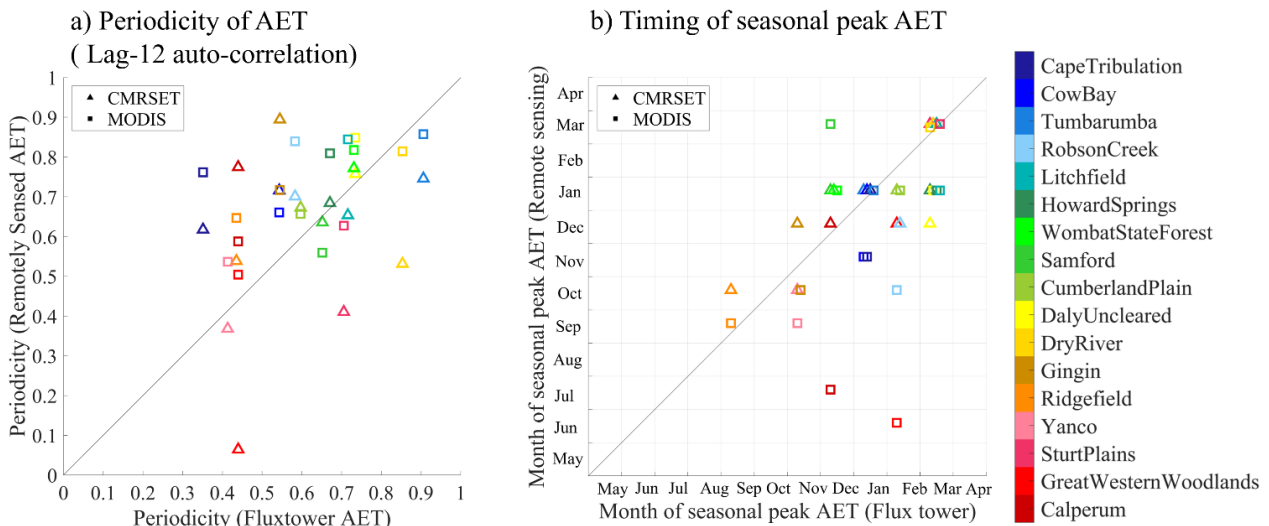
Figure 4: Comparison of seasonal AET signatures, a) Periodicity of AET (Lag-12 auto-correlation), b) Timing of seasonal peak, between remotely sensed AET (MODIS and CMRSET AET) and flux tower AET. Note that Figure 4b values take integer values only (i.e., either one calendar month or the next), leading to several points overlying the same plotting position; to make every point visible we subject each point to a jitter (i.e., a unique offset within the same grid cell).

3.3 Monthly AET signatures

230 Figure 5 quantifies and compares monthly AET signatures using $AET_{Fluxtower}$ and AET_{RS}. Figure 5a shows a lower $CV_{monthly}$ at less arid flux towers such as Cape Tribulation, Cow Bay, and Robson Creek, with most other flux towers grouping tightly between CV values of 0.3 and 0.6, while Sturt Plains is a clear outlier at 0.9. $CV_{monthly}$ from CMRSET and MODIS AET do not show much overall bias relative to $AET_{Fluxtower}$, yet the match with observed is very poor, with considerable scatter due to overestimation and underestimation of $CV_{monthly}$, depending on site.

235 Regarding *water stress* (WS), Figure 5b shows how WS increases with aridity, as expected. WS from CMRSET and MODIS AET is moderately well predicted except for wet flux towers, which are underestimated. It is possible that this is due to errors or biases in PET (recall that Morton's Wet Environment PET was used), which may be less of an issue when PET is clearly greater than AET, whereas in cases where they are similar PET errors may be more important. Figure 5c shows the *AET asynchronicity to PET* (AAP) that incorporates differences in phases between AET and PET timeseries. Results show that

240 both $AET_{Fluxtower}$ and AET_{RS} are asynchronous with PET (i.e., $APP > 0$) for all the sites. However, at wetter sites, AET is more synchronous with PET showing smaller APP values (i.e., smaller APP indicates closer synchronicity to PET), perhaps suggesting few temporal gaps in water availability, but increasing with aridity index (except at Calperum and Great Western Woodlands sites). Furthermore, the results show separation between remotely sensed products, with MODIS showing more AAP while CMRSET showing lower AAP compared to flux tower AAP for sites exhibiting higher than average asynchronicity.

245 3.4 Event-scale AET signatures

Figure 6 shows the index of AET responsiveness to a rainfall event (R). Recall that such information is unavailable for RS data due to its longer timestep. The R of zero indicates no correlation between rainfall event and the subsequent AET, and Figure 6 shows no discernible correlation between the magnitude of a rainfall event (i.e., > 5mm/day in this example) and the subsequent AET on either the rain day or thereafter (i.e., maximum of 10 days window in this example) at the majority of the

250 flux tower sites, and even a slightly negative correlation, perhaps suggesting that rain days might be followed by cloudy weather that suppresses AET.

### 3.5 Traditional efficiency metrics

Figure 7 shows a range of commonly used efficiency metrics such as NSE, KGE, and the sub-components of KGE, namely, the ratio of standard deviations (α), the ratio of means (β), and the Pearson correlation coefficient (r), calculated using monthly

255 MODIS and CMRSET AET with flux tower AET. The distribution of NSE (median: -0.11) from MODIS AET indicates a poor prediction of $AET_{Fluxtower}$ on the monthly scale. In contrast, the distribution of NSE from CMRSET AET shows a positive, but still close to zero, median value of 0.14, implying better performance than MODIS but still overall poor performance.

For KGE, the median KGE values across flux tower sites for monthly MODIS and CMRSET AET are 0.45 and 0.53, respectively. The sub-components of KGE, such as α shows closer variability in MODIS AET (median α = 1.07) and in

Hydrology and
Earth System
Sciences
Discussions
Open Access
EGU

260   CMRSET (median α = 0.94) compared to flux tower estimates. The β component of KGE shows a lower mean in MODIS
      AET (median β = 0.77) and a slightly higher mean in CMRSET (median β = 1. 07) compared to flux tower estimates. The r
      component of KGE shows a relatively similar correlation for both MODIS AET (median r = 0.77) and CMRSET (median r =
      0.69) with $AET_{Fluxtower}$. Although these components of KGE provide valuable information about the ability of AET_{RS} to capture
      dynamics from $AET_{Fluxtower}$, this information is diluted in the final KGE value. Figure S1 in the supplementary information
265   shows the traditional efficiency metric values at each flux tower site.
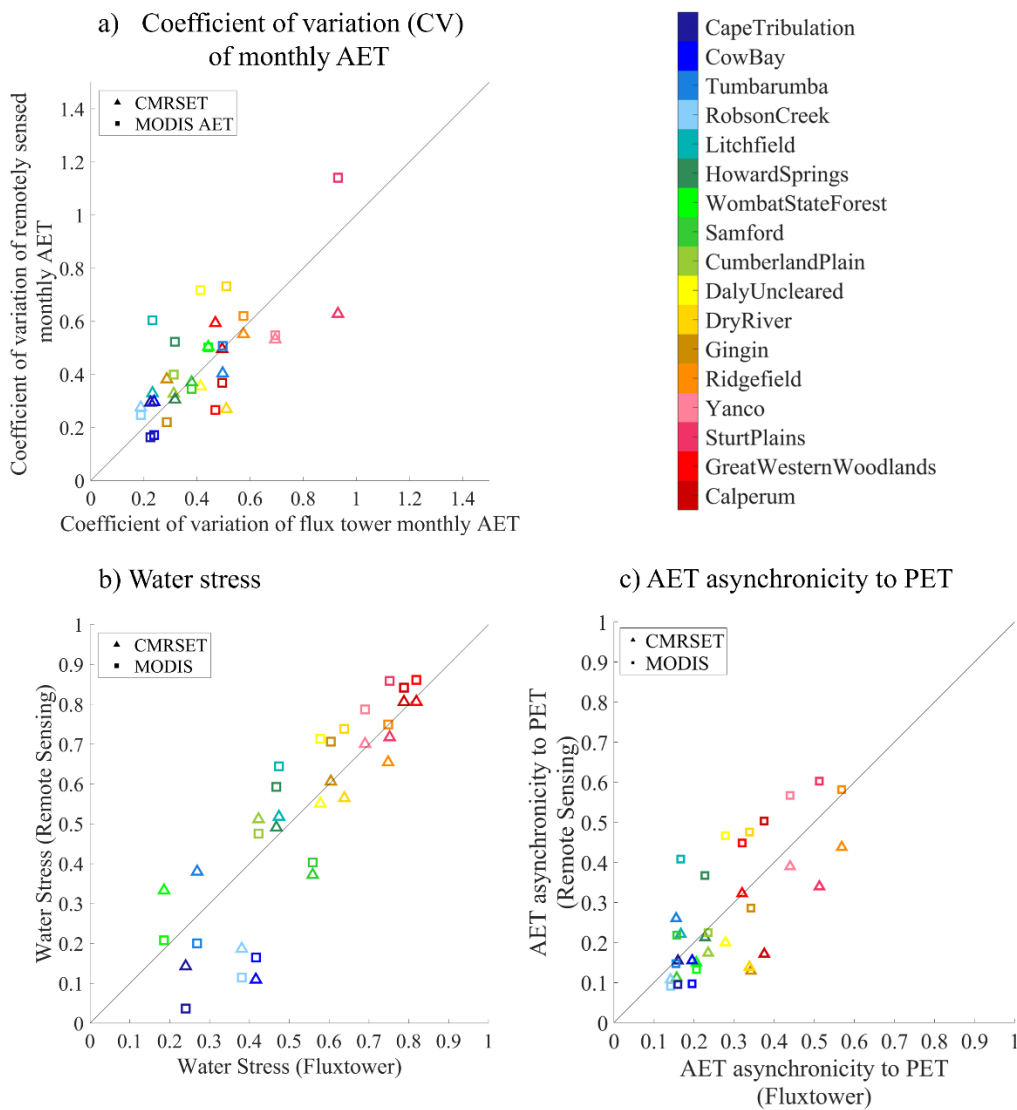

Figure 5: Comparison of monthly signatures; a) Coefficient of variation of monthly AET, b) Water stress, and c) AET asynchronicity to PET, between remotely sensed AET (MODIS and CMRSET) and flux tower AET.
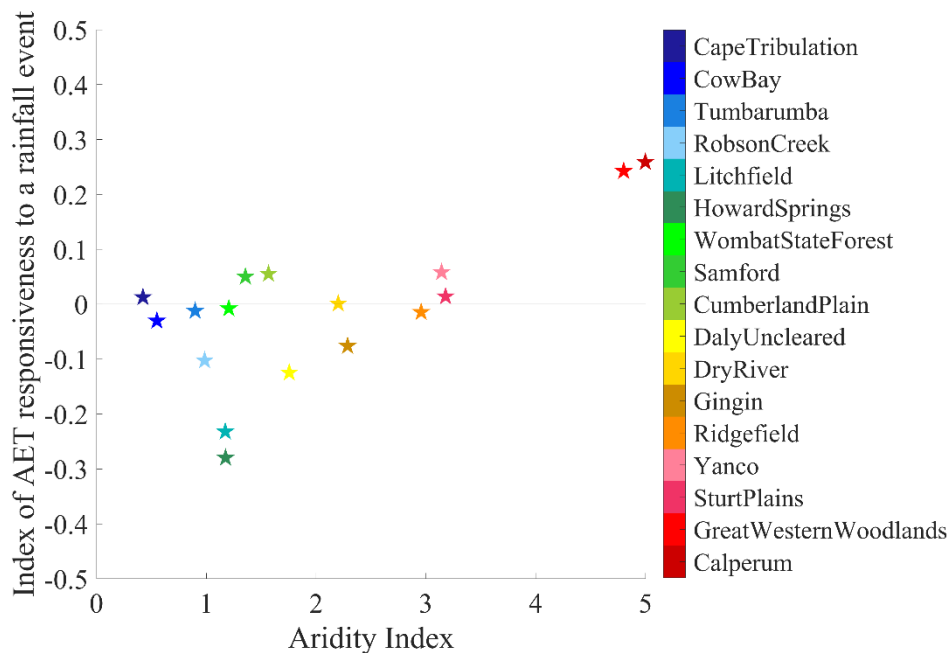
Figure 6: Index of AET responsiveness to rainfall vs. aridity index at flux tower sites. (Note that the index of zero indicates no correlation between rainfall event and the subsequent AET).
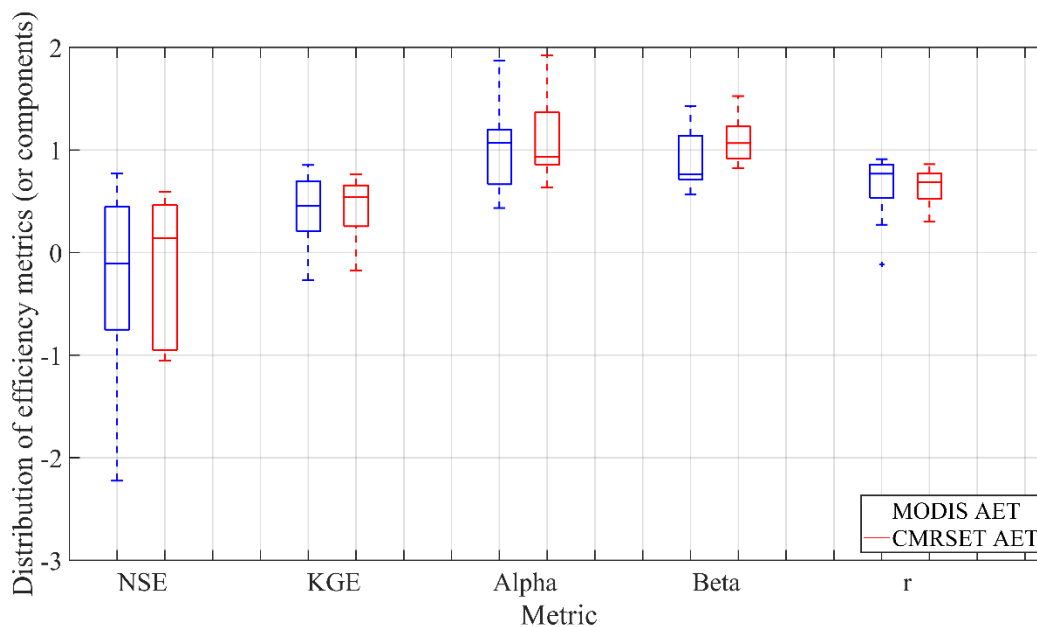
Figure 7: Distribution of conventional efficiency metrics, all calculated on a monthly timestep: 1) Nash Sutcliffe efficiency (NSE), 2) Kling Gupta Efficiency (KGE), 3) Alpha (α – ratio of standard deviations), 4) Beta (β – ratio of means), and r (r – Pearson correlation coefficient), calculated using monthly MODIS and CMRSET AET with flux tower AET (Note that there are two outliers not shown in the NSE calculated for MODIS and CMRSET, which are lower than -3).

14

4 Discussion

280 This study developed evapotranspiration signatures at various temporal scales and used them to evaluate remotely sensed AET information against flux towers. The study provides a basis for exploring what sort of signatures might be useful when investigating and characterising AET behaviours, with applications across other domains, such as characterising catchment processes and critiquing hydrological models.

4.1 Value of AET signatures over aggregate measures of performance

AET signatures introduced in this analysis offer comprehensive behavioural insights into AET to complement existing suites
285 of indices for streamflow and, to a lesser extent, groundwater. A key benefit of these signatures is their capacity to characterise different aspects of AET dynamics, allowing the quantification of nuanced aspects that can be discerned through visual inspection but, without signatures, are not easily defined numerically. Some examples are given in Table 3.

Table 3: Example of aspects of AET dynamics that can be discerned via visual inspection of timeseries (Figure 2) and are subsequently reflected in signature results (Figure 4 & 5)

Flux tower	Aspects of AET dynamics based on visual inspection	Corresponding signature results
Calperum	CMRSET closely synchronizes with PET variability	AET asynchronicity to PET(AAP) is low (0.17; note a value of zero would mean perfect synchronicity)
	The seasonal variation in MODIS is shifted (peaks are too early)	Timing of seasonal peaks (TSP) indicates earlier peak (July for MODIS compared to December for CMRSET and fluxtower)
Gingin	The seasonal variation in fluxtower AET is offset with PET	Fluxtower AAP is relatively higher (0.34) showing the asynchronicity with PET
	CMRSET closely synchronizes with PET variability.	CMRSET AAP is low (0.12)
Cumberland Plain	Clear and regular seasonal cycle is observed in fluxtower and RS AET	Periodicity ($P_{12month}$) is greater than 0.6 for fluxtower and RS AET
	Fluxtower and RS AET are mostly synchronized	TSP is same for MODIS and CMRSET (January) and only slightly different for fluxtower (February)
Wombat State Forest	Clear and regular seasonal cycle is observed in fluxtower and RS AET	$P_{12month}$ is greater than 0.73 for fluxtower and RS AET
	Clear and somewhat high temporal variability of monthly AET is observed in fluxtower and RS AET	Coefficient of variation (CV) is greater than 0.44 for fluxtower and RS AET

Hydrology and
Earth System
Sciences
Discussions

EGU
Open Access

Howard Springs	Relatively high temporal variability of monthly AET is observed in fluxtower and RS AET	CV is higher in MODIS (0.52) compared to fluxtower AET (0.32) and CMRSET (0.31)
	fluxtower and RS AET are mostly synchronized.	TSP is same for MODIS and CMRSET (January) and different for fluxtower (March)
Robson Creek	Lower temporal variability of monthly AET is observed in fluxtower AET compared to RS AET	CV is low in fluxtower AET (0.18) compared to CMRSET (0.27) and MODIS (0.24)
	RS AET is more responsive to and synchronizes with PET than fluxtower AET	Flux tower water stress (WS) is higher (0.38) compared to CMRSET (0.17) and MODIS (0.11)

290

This capacity for nuanced characterisation in AET signatures contrasts with traditional fit/performance metrics such as NSE and KGE. As mentioned in the introduction, these commonly used performance metrics are often applied to quantify hydrological model performances but may obscure specific behavioural information (McMillan, 2021; Wagener & Gupta, 2005). For example, the NSE calculated using monthly MODIS and CMRSET AET at some flux tower sites showed negative

295 values, indicating bad predictive skills, whereas the KGE calculated using both the AET$_{RS}$ tended to show some predictive skills over flux tower observations. However, both of these conventional performance metrics fail to identify what aspects of AET in remote sensing products have led to poor prediction of AET$_{Fluxtower}$. Even though the subcomponents of KGE, such as the ratio of standard deviation, the ratio of mean, and the Pearson correlation coefficient, provided valuable information about the ability of these two AET$_{RS}$ products to capture AET dynamics compared to AET$_{Fluxtower}$, the final KGE value dilute this

300 information. Therefore, incorporating AET signatures into applications such as hydrological model calibration and evaluation could lead to more accurate and realistic outcomes.

4.2 Insights into actual evapotranspiration behaviour at Australian flux tower sites

This study confirms various anticipated AET behaviours at flux tower sites in Australia across different temporal scales. For example, the $\widehat{AET}_{annual}$ increased as the aridity index decreased as expected, indicating that less arid flux towers have a higher

305 $\widehat{AET}_{annual}$, whereas more arid flux towers have a lower $\widehat{AET}_{annual}$. However, the CV_{annual} across flux tower sites was low (range of 0-0.2 at 14 out of 17 sites), regardless of their aridity index. This finding is consistent with the relatively constant annual AET variability over time, as reported by Gardiya Weligamage et al. (2023). In terms of $CV_{monthly}$ of flux tower AET, a higher degree of AET fluctuation was observed compared to the annual scale; however, flux towers situated in temperate climates with dry winters and hot summers (e.g., Cape Tribulation, Cow Bay, and Robson Creek) exhibited lower monthly

310 variability. As expected, WS at flux towers largely increased with increased aridity. Regarding seasonal AET behaviour, the TSP of flux tower AET was identified between November and March. Regarding the $P_{12month}$ of flux tower AET, no distinct relationship was found between periodicity and the aridity index. At the event scale, most flux towers did not show a discernible correlation between rainfall events and subsequent AET events. Therefore, at this stage, the '*index of AET responsiveness to*

a rainfall event' signature does not appear to add significant value in this AET signature analysis. However, we employed this
315 event-scale signature to evaluate commonly used conceptual rainfall-runoff model performances in a companion paper (Gardiya Weligamage et al., 2024), and the models were found to be very biased in this signature. Therefore, this event-scale signature adds value in constraining models or exploring model deficiency. Furthermore, this event-scale signature is particularly noteworthy, as it highlights a distinct aspect of AET dynamics not previously quantified. As McMillan, (2020) confirmed, no signature (even an indirect AET behaviour explanation using hydrological signatures) was previously identified
320 for assessing AET at the event scale.

4.3 Implications for quality of remotely sensed actual evapotranspiration

The eight AET signatures proposed in this study are used to highlight the strengths and weaknesses of two AET_{RS} products (i.e., MODIS AET and CMRSET) on multiple aspects by assessing their AET signatures with those obtained from flux tower observations. Given that it seems increasingly common for studies (particularly modelling studies) to uncritically adopt AET_{RS}
325 products, these findings underscore the deficiencies in AET_{RS} data and pinpoint several specific aspects of failure. Thus, we emphasize the importance of investigating AET_{RS} data prior to use in any other applications, such as rainfall-runoff modelling. More specifically, most signatures, such as monthly and seasonal (except periodicity from MODIS monthly AET) AET signatures, reveal that AET_{RS} is generally unbiased compared to $AET_{Fluxtower}$. However, the wide scatter observed in the AET signatures underscores the challenge of reproducing the dynamics captured by flux tower data. This wide scatter was seen in
330 several signatures such as $CV_{monthly}$, *AAP*, $P_{12month}$*, and TSP*. At the annual scale, RS-derived AET signatures of $\widehat{AET}_{annual}$ and $CV_{monthly}$ showed underestimation (negative bias) relative to flux towers. At the seasonal scale, challenges were particularly pronounced with the MODIS AET, which exhibited offsets in *TSP*, while being overly periodic compared to flux tower data. Therefore, caution should be exercised when extracting seasonal information from MODIS AET. Conversely, the regionally developed CMRSET product tended to align comparatively better with the *TSP* observed by flux towers, likely because the
335 CMRSET model was calibrated only to flux tower sites in Australia (Guerschman et al., 2022), in contrast to MODIS which is globally calibrated and thus has less Australian focus. Our findings concur with Guerschman et al. (2022), who reported that the calibrated CMRSET model performs better than MODIS AET (i.e., MOD16A2). However, CMRSET exhibited greater scatter in terms of periodicity, highlighting issues with seasonal consistency.

4.4 Limitations and future studies

340 While this study assessed these signatures calculated using $AET_{Fluxtower}$ estimates and compared them with those calculated using AET_{RS} estimates, there are uncertainties associated with flux measurement errors and spatial representativeness of both estimates. In this study, we assumed the $AET_{Fluxtower}$ to be robust and compared the AET signatures calculated using them with those calculated using remotely sensed products. However, these flux towers may be subjected to errors in energy closure in the eddy covariance method due to conditions such as weak turbulence or systematic flux leakage on hillslopes (Chen et al.,
345 2011; Wilson et al., 2002). Moreover, as mentioned, there can be differences in AET signatures due to the different spatial

footprints of observation between AET_{RS} and $AET_{Fluxtower}$. Viewing this study as starting point for the study of AET signatures, future studies can expand or modify these signatures in order to best capture AET behaviours, including on other continents, and can be employed in hydrological model calibration and evaluation to represent AET processes realistically.

5. Conclusion

350 This study proposed eight AET signatures to explore AET behaviours at different temporal scales, expanding upon hydrological signature studies and providing comprehensive insights into AET dynamics. The AET signatures calculated from flux towers in Australia were consistent with anticipated AET behaviour, and their comparison with signatures derived from remotely sensed AET data highlights the strengths and weaknesses of RS information. In a broader context, the remotely sensed products used in this study show significant scatter around the flux tower values, signalling caution regarding their

355 capacity to mimic observed AET behaviours accurately. Therefore, future studies are encouraged to leverage these AET signatures to evaluate remotely sensed products before their adopted and to better extract and improve information for activities such as hydrological modelling.

Data availability

The actual evapotranspiration data extracted from Ozflux sites and remotely sensed products are available at
360 https://doi.org/10.5281/zenodo.14226802.

Author contribution

Hansini Gardiya Weligamage: Conceptualization, Data curation, Formal analysis, Investigation, Methodology, Validation, Visualization, Writing – original draft preparation, Writing – review and editing.
Keirnan Fowler: Conceptualization, Methodology, Funding acquisition, Supervision, Writing – review and editing
365 Margarita Saft: Conceptualization, Methodology, Funding acquisition, Supervision, Writing – review and editing
Tim Peterson: Conceptualization, Methodology, Funding acquisition, Supervision, Project administration, Writing – review and editing
Dongryeol Ryu: Conceptualization, Methodology, Supervision, Writing – review and editing
Murray Peel: Conceptualization, Methodology, Funding acquisition, Supervision, Project administration, Writing – review
370 and edit

Competing interests

The authors declare that they have no conflict of interest.

Hydrology and
Earth System
Sciences
Discussions

Open Access

EGU

References

Abbott, B. W., Bishop, K., Zarnetske, J. P., Minaudo, C., Chapin, F. S., Krause, S., Hannah, D. M., Conner, L., Ellison, D., Godsey, S. E., Plont, S., Marçais, J., Kolbe, T., Huebner, A., Frei, R. J., Hampton, T., Gu, S., Buhman, M., Sara Sayedi, S., …

380 Pinay, G.: Human domination of the global water cycle absent from depictions and perceptions. Nature Geoscience, 12(7), 533–540. https://doi.org/10.1038/s41561-019-0374-y, 2019.

Addor, N., Nearing, G., Prieto, C., Newman, A. J., Le Vine, N., & Clark, M. P.: A Ranking of Hydrological Signatures Based on Their Predictability in Space. Water Resources Research, 54(11), 8792–8812. https://doi.org/10.1029/2018WR022606, 2018.

385 Araki, R., Branger, F., Wiekenkamp, I., & McMillan, H.: A signature-based approach to quantify soil moisture dynamics under contrasting land-uses. Hydrological Processes, 36(4). https://doi.org/10.1002/hyp.14553, 2022.

Arndt, S., Hinko-Najera, N., & Griebel, A.: Wombat State Forest Flux Data Release 2024_v1. Version 2024_v1. Terrestrial Ecosystem Research Network. (Dataset), 2024.

Avanzi, F., Rungee, J., Maurer, T., Bales, R., Ma, Q., Glaser, S., & Conklin, M.: Climate elasticity of evapotranspiration shifts

390 the water balance of Mediterranean climates during multi-year droughts. Hydrology and Earth System Sciences, 24(9), 4317–4337. https://doi.org/10.5194/hess-24-4317-2020, 2020.

Baker, J. C. A., Garcia-Carreras, L., Gloor, M., Marsham, J. H., Buermann, W., da Rocha, H. R., Nobre, A. D., de Araujo, A. C., & Spracklen, D. V.: Evapotranspiration in the Amazon: spatial patterns, seasonality, and recent trends in observations, reanalysis, and climate models. Hydrology and Earth System Sciences, 25(4), 2279–2300, https://doi.org/10.5194/hess-25-

395 2279-2021, 2021.

Beringer, J., Hutley, L., & Northwood, M.: Daly Uncleared Flux Data Release 2024_v1. Version 2024_v1. Terrestrial Ecosystem Research Network. (Dataset), 2024a.

Beringer, J., Hutley, L., & Northwood, M.: Dry River Flux Data Release 2024_v1. Version 2024_v1. Terrestrial Ecosystem Research Network. (Dataset), 2024b.

400 Beringer, J., Hutley, L., & Northwood, M.: Howard Springs Flux Data Release 2024_v1. Version 2024_v1. Terrestrial Ecosystem Research Network. (Dataset), 2024c.

Beringer, J., Hutley, L., & Northwood, M.: Litchfield Flux Data Release 2024_v1. Version 2024_v1. Terrestrial Ecosystem Research Network. (Dataset), 2024d.

Beringer, J., Hutley, L., & Northwood, M.: Sturt Plains Flux Data Release 2024_v1. Version 2024_v1. Terrestrial Ecosystem
405 Research Network. (Dataset), 2024e.

Beringer, J., Lardner, T., & Moore, C.: Ridgefield Flux Data Release 2024_v1. Terrestrial Ecosystem Research Network.
(Dataset), 2024.

Beringer, J., Walker, J., Rudiger, C., Daly, E., Dumedah, G., Monerris-Belda, A., Yee, M. S., Winston, F., Lubcke, T., &
Hocking, D.: Yanco Flux Data Release 2024_v1. Version 2024_v1. Terrestrial Ecosystem Research Network. (Dataset), 2024.

410 Chen, B., Coops, N. C., Fu, D., Margolis, H. A., Amiro, B. D., Barr, A. G., Black, T. A., Arain, M. A., Bourque, C. P.-A., &
Flanagan, L. B.: Assessing eddy-covariance flux tower location bias across the Fluxnet-Canada Research Network based on
remote sensing and footprint modelling. Agricultural and Forest Meteorology, 151(1), 87–100,
https://doi.org/10.1016/j.agrformet.2010.09.005, 2011.

Chu, H., Luo, X., Ouyang, Z., Chan, W. S., Dengel, S., Biraud, S. C., Torn, M. S., Metzger, S., Kumar, J., Arain, M. A.,
415 Arkebauer, T. J., Baldocchi, D., Bernacchi, C., Billesbach, D., Black, T. A., Blanken, P. D., Bohrer, G., Bracho, R., Brown,
S., … Zona, D.: Representativeness of Eddy-Covariance flux footprints for areas surrounding AmeriFlux sites. Agricultural
and Forest Meteorology, 301–302(February). https://doi.org/10.1016/j.agrformet.2021.108350, 2021.

Clausen, B., & Biggs, B. J. F.: Flow variables for ecological studies in temperate streams: groupings based on covariance.
Journal of Hydrology, 237(3–4), 184–197. https://doi.org/10.1016/S0022-1694(00)00306-1, 2000.

420 Doody, T. M., Benyon, R. G., & Gao, S.: Fine scale 20-year timeseries of plantation forest evapotranspiration for the Lower
Limestone Coast. Hydrological Processes, 37(3), e14836, https://doi.org/10.1002/hyp.14836, 2023.

Finnigan, J.: AN INTRODUCTION TO FLUX MEASUREMENTS IN DIFFICULT CONDITIONS. Ecological Applications,
18(6), 1340–1350. https://doi.org/10.1890/07-2105.1, 2008.

Gaona, J., Quintana-Seguí, P., Escorihuela, M. J., Boone, A., & Llasat, M. C.: Interactions between precipitation,
425 evapotranspiration and soil-moisture-based indices to characterize drought with high-resolution remote sensing and land-
surface model data. Natural Hazards and Earth System Sciences, 22(10), 3461–3485, https://doi.org/10.5194/nhess-22-3461-
2022, 2022.

Gardiya Weligamage, H., Fowler, K., Peterson, T. J., Saft, M., Peel, M. C., & Ryu, D.: Partitioning of Precipitation Into
Terrestrial Water Balance Components Under a Drying Climate. Water Resources Research, 59(5), e2022WR033538.
430 https://doi.org/10.1029/2022WR033538, 2023.

Gardiya Weligamage, H., Fowler, K., Saft, M., Peterson, T., Ryu, D., & Peel, M.: Assessing evapotranspiration realism in
rainfall-runoff models using evapotranspiration signatures [submitted]. Hydrology and Earth System Sciences, 2024.

Grace, P., Rowlings, D., Grace, L., & Tucker, D.: Samford Ecological Research Facility Flux Data Release 2024_v1.
Terrestrial Ecosystem Research Network. (Dataset), 2024.

435 Guerschman, J. P., McVicar, T. R., Vleeshower, J., Van Niel, T. G., Peña-Arancibia, J. L., & Chen, Y.: Estimating actual
evapotranspiration at field-to-continent scales by calibrating the CMRSET algorithm with MODIS, VIIRS, Landsat and
Sentinel-2 data. Journal of Hydrology, 605(December 2021), 127318. https://doi.org/10.1016/j.jhydrol.2021.127318, 2022a.

Gupta, H. V., Wagener, T., & Liu, Y.: Reconciling theory with observations: Elements of a diagnostic approach to model evaluation. Hydrological Processes, 22(18), 3802–3813. https://doi.org/10.1002/hyp.6989, 2008.

440   Heudorfer, B., Haaf, E., Stahl, K., & Barthel, R.: Index-Based Characterization and Quantification of Groundwater Dynamics. Water Resources Research, 55(7), 5575–5592. https://doi.org/10.1029/2018WR024418, 2019.

Isaac, P., Cleverly, J., McHugh, I., van Gorsel, E., Ewenz, C., & Beringer, J.: OzFlux data: network integration from collection to curation. Biogeosciences, 14(12), 2903–2928. https://doi.org/10.5194/bg-14-2903-2017, 2017.

Kiraz, M., Coxon, G., & Wagener, T.: A Signature-Based Hydrologic Efficiency Metric for Model Calibration and Evaluation

445   in Gauged and Ungauged Catchments. Water Resources Research, 59(11). https://doi.org/10.1029/2023WR035321, 2023.

Klemeš, V. (1983). Conceptualization and scale in hydrology. Journal of Hydrology, 65(1–3), 1–23.

Koster, R. D., & Suarez, M. J.: Soil Moisture Memory in Climate Models. Journal of Hydrometeorology, 2(6), 558–570. https://doi.org/10.1175/1525-7541(2001)002<0558:SMMICM>2.0.CO;2, 2001.

Liddell, M., & Weigand, N.: Cape Tribulation Flux Data Release 2024_v1. Version 2024_v1. Terrestrial Ecosystem Research

450   Network. (Dataset), 2024a.

Liddell, M., & Weigand, N.: Cow Bay Flux Data Release 2024_v1. Version 2024_v1. Terrestrial Ecosystem Research Network. (Dataset) 2024b.

Liddell, M., & Weigand, N.: Robson Creek Flux Data Release 2024_v1. Version 2024_v1. Terrestrial Ecosystem Research Network. (Dataset), 2024c.

455   Macfarlane, C., Prober, S., & Wiehl, G.: Great Western Woodlands Flux Data Release 2024_v1. Version 2024_v1. Terrestrial Ecosystem Research Network. (Dataset), 2024.

McMillan, H.: Linking hydrologic signatures to hydrologic processes: A review. Hydrological Processes, 34(6), 1393–1409. https://doi.org/10.1002/hyp.13632, 2020.

McMillan, H., Gueguen, M., Grimon, E., Woods, R., Clark, M., & Rupp, D. E.: Spatial variability of hydrological processes

460   and model structure diagnostics in a 50 km2 catchment. Hydrological Processes, 28(18), 4896–4913. https://doi.org/10.1002/hyp.9988, 2014.

McMillan, H. K.: A review of hydrologic signatures and their applications. WIREs Water, 8(1), 1–23. https://doi.org/10.1002/wat2.1499, 2021.

McVicar, T., Vleeshouwer, J., Van Niel, T., & Guerschman, J.: Actual Evapotranspiration for Australia using CMRSET

465   algorithm. Terrestrial Ecosystem Research Network. (Dataset), 2022.

Meyer, W., Ewenz, C., Koerber, G., & Lubcke, T.: Calperum Chowilla Flux Data Release 2024_v1. Version 2024_v1. Terrestrial Ecosystem Research Network. (Dataset), 2024.

Morton, F. I.: Operational estimates of areal evapotranspiration and their significance to the science and practice of hydrology. Journal of Hydrology, 66(1-4), 1–76. https://doi.org/10.1016/0022-1694(83)90177-4, 1983.

470   Olden, J. D., & Poff, N. L.: Redundancy and the choice of hydrologic indices for characterizing streamflow regimes. River Research and Applications, 19(2), 101–121. https://doi.org/10.1002/rra.700, 2003.

Pendall, E., Griebel, A., Barton, C., & Metzen, D.: Cumberland Plain Flux Data Release 2024_v1. Version 2024_v1. Terrestrial Ecosystem Research Network. (Dataset), 2024.

Peterson, T. J., & Fulton, S.: Joint Estimation of Gross Recharge, Groundwater Usage, and Hydraulic Properties within HydroSight. Groundwater, 57(6), 860–876. https://doi.org/10.1111/gwat.12946, 2019.

Peterson, T. J., Saft, M., Peel, M. C., & John, A.: Watersheds may not recover from drought. Science, 372(6543), 745–749, https://doi.org/10.1126/science.abd5085, 2021.

Rungee, J., Bales, R., & Goulden, M.: Evapotranspiration response to multiyear dry periods in the semiarid western United States. Hydrological Processes, 33(2), 182–194. https://doi.org/10.1002/hyp.13322, 2019.

Running, S., Mu, Q., Zhao, M., & Moreno, A.: MODIS/Terra Net Evapotranspiration Gap-Filled 8-Day L4 Global 500m SIN Grid V061 (Dataset). NASA EOSDIS Land Processes Distributed Active Archive Center, Accessed April 30, 2024. https://doi.org/10.5067/MODIS/MOD16A2GF.061, 2021.

Safeeq, M., & Hunsaker, C. T.: Characterizing Runoff and Water Yield for Headwater Catchments in the Southern Sierra Nevada. JAWRA Journal of the American Water Resources Association, 52(6), 1327–1346. https://doi.org/10.1111/1752-1688.12457, 2016.

Salazar-Martínez, D., Holwerda, F., Holmes, T. R. H., Yépez, E. A., Hain, C. R., Alvarado-Barrientos, S., Ángeles-Pérez, G., Arredondo-Moreno, T., Delgado-Balbuena, J., & Figueroa-Espinoza, B.: Evaluation of remote sensing-based evapotranspiration products at low-latitude eddy covariance sites. Journal of Hydrology, 610, 127786, https://doi.org/10.1016/j.jhydrol.2022.127786, 2022.

Schwab, M., Klaus, J., Pfister, L., & Weiler, M.: Diel discharge cycles explained through viscosity fluctuations in riparian inflow. Water Resources Research, 52(11), 8744–8755. https://doi.org/10.1002/2016WR018626, 2016.

Silberstein, R., Lambert, P., Lardner, T., & Macfarlane, C.: Gingin Flux Data Release 2024_v1. Version 2024_v1. Terrestrial Ecosystem Research Network. (Dataset), 2024.

Stol, J., & Kitchen, M.: Tumbarumba Flux Data Release 2024_v1. Version 2024_v1. Terrestrial Ecosystem Research Network. (Dataset), 2024.

Teluguntla, P., Ryu, D., George, B., & Walker, J. P.: Multidecadal Trend of Basin-Scale Evapotranspiration Estimated Using AVHRR Data in the Krishna River Basin, India. Vadose Zone Journal, 12(3), vzj2012.0118. https://doi.org/10.2136/vzj2012.0118, 2013.

Wagener, T., & Gupta, H. V.: Model identification for hydrological forecasting under uncertainty. Stochastic Environmental Research and Risk Assessment, 19, 378–387, https://doi.org/10.1007/s00477-005-0006-5, 2005.

Westerberg, I. K., Guerrero, J. L., Younger, P. M., Beven, K. J., Seibert, J., Halldin, S., Freer, J. E., & Xu, C. Y.: Calibration of hydrological models using flow-duration curves. Hydrology and Earth System Sciences, 15(7), 2205–2227. https://doi.org/10.5194/hess-15-2205-2011, 2011.

Wilson, K., Goldstein, A., Falge, E., Aubinet, M., Baldocchi, D., Berbigier, P., Bernhofer, C., Ceulemans, R., Dolman, H., &
505 Field, C.: Energy balance closure at FLUXNET sites. Agricultural and Forest Meteorology, 113(1–4), 223–243,
https://doi.org/10.1016/S0168-1923(02)00109-0, 2002.

Wondzell, S. M., Gooseff, M. N., & McGlynn, B. L.: An analysis of alternative conceptual models relating hyporheic exchange
flow to diel fluctuations in discharge during baseflow recession. Hydrological Processes, 24(6), 686–694.
https://doi.org/10.1002/hyp.7507, 2010.

510 Wrede, S., Fenicia, F., Martínez-Carreras, N., Juilleret, J., Hissler, C., Krein, A., Savenije, H. H. G., Uhlenbrook, S., Kavetski,
D., & Pfister, L.: Towards more systematic perceptual model development: a case study using 3 Luxembourgish catchments.
Hydrological Processes, 29(12), 2731–2750. https://doi.org/10.1002/hyp.10393, 2015.

Xu, Z., Zhang, Y., Zhang, X., Ma, N., Tian, J., Kong, D., & Post, D.: Bushfire-Induced Water Balance Changes Detected by
a Modified Paired Catchment Method. Water Resources Research, 58(11), e2021WR031013,
515 https://doi.org/10.1029/2021WR031013, 2022.

Yan, N., Tian, F., Wu, B., Zhu, W., & Yu, M.: Spatiotemporal analysis of actual evapotranspiration and its causes in the Hai
Basin. Remote Sensing, 10(2). https://doi.org/10.3390/rs10020332, 2018.

Zhang, K., Kimball, J. S., Nemani, R. R., & Running, S. W.: A continuous satellite-derived global record of land surface
evapotranspiration from 1983 to 2006. Water Resources Research, 46(9), 1–21. https://doi.org/10.1029/2009WR008800, 2010.

520 Zhang, K., Kimball, J. S., & Running, S. W.: A review of remote sensing based actual evapotranspiration estimation. In Wiley
Interdisciplinary Reviews: Water (Vol. 3, Issue 6, pp. 834–853). John Wiley and Sons Inc. https://doi.org/10.1002/wat2.1168,
2016.